ORIGINAL ARTICLE

Thalamo-Cortical Disruption Contributes to Short-Term Memory Deficits in Patients with Medial Temporal Lobe Damage

Natalie L. Voets[1,2], Ricarda A. L. Menke[1], Saad Jbabdi[1], Masud Husain[1,2,3], Richard Stacey[4], Katherine Carpenter[5], and Jane E. Adcock[1,2]

[1]FMRIB Centre, Nuffield Department of Clinical Neurosciences, [2]Epilepsy Research Group, Nuffield Department of Clinical Neurosciences, University of Oxford, John Radcliffe Hospital, Oxford OX3 9DU, UK, [3]Department of Experimental Psychology, University of Oxford, Oxford OX1 3UD, UK, [4]Department of Neurosurgery and [5]Russell Cairns Unit, John Radcliffe Hospital, Oxford OX3 9DU, UK

Address correspondence to Natalie L. Voets, FMRIB Centre, University of Oxford, John Radcliffe Hospital, Headington, Oxford OX3 9DU, UK. Email: natalie.voets@ndcn.ox.ac.uk

Abstract

Short-term (STM) and long-term memory (LTM) have largely been considered as separate brain systems reflecting fronto-parietal and medial temporal lobe (MTL) functions, respectively. This functional dichotomy has been called into question by evidence of deficits on aspects of working memory in patients with MTL damage, suggesting a potentially direct hippocampal contribution to STM. As the hippocampus has direct anatomical connections with the thalamus, we tested the hypothesis that damage to thalamic nuclei regulating cortico-cortical interactions may contribute to STM deficits in patients with hippocampal dysfunction. We used diffusion-weighted magnetic resonance imaging-based tractography to identify anatomical subdivisions in patients with MTL epilepsy. From these, we measured resting-state functional connectivity with detailed cortical divisions of the frontal, temporal, and parietal lobes. Whereas thalamo-temporal functional connectivity reflected LTM performance, thalamo-prefrontal functional connectivity specifically predicted STM performance. Notably, patients with hippocampal volume loss showed thalamic volume loss, most prominent in the pulvinar region, not detected in patients with normal hippocampal volumes. Aberrant thalamo-cortical connectivity in the epileptic hemisphere was mirrored in a loss of behavioral association with STM performance specifically in patients with hippocampal atrophy. These findings identify thalamo-cortical disruption as a potential mechanism contributing to STM deficits in the context of MTL damage.

Key words: epilepsy, functional connectivity, hippocampus, memory, thalamus

Introduction

Since the discovery that medial temporal lobe (MTL) damage can induce profound amnesia while leaving immediate recall intact (Corkin 1984), short-term and long-term memory (STM and LTM) have been largely considered as separate functional brain systems (Wickelgren 1968; Shallice and Warrington 1970). Complementing a LTM circuit in the temporal lobe, the short-term retention and manipulation of information in "working" memory

has been allocated to a primarily pre-fronto-parietal network (Goldman-Rakic 1988; Owen et al. 1999; Todd and Marois 2004).

More recently, a direct contribution of MTL structures to working memory has been advanced, based on MTL neural activity during STM tasks (Ranganath and D'Esposito 2001; Oztekin et al. 2010) and memory failures even across short delays in MTL-damaged patients (Olson, Moore, et al. 2006; Olson, Page, et al. 2006; Hartley et al. 2007; Pertzov et al. 2013). These data conflict with other demonstrations of preserved STM despite extensive hippocampal lesions in human patients (Jeneson et al. 2010; Baddeley et al. 2011) and animal models (Alvarez et al. 1994). To reconcile these findings, it is argued that relative hippocampal involvement might reflect how much task manipulations (i) exceed immediate memory capacity (Jeneson and Squire 2012) or (ii) require complex stimulus associations (Yonelinas 2013). However, uncertainty concerning the extent of MTL damage (Baddeley et al. 2010) poses major interpretational challenges in hippocampal damage patients.

Indeed, the MTL has extensive connections including with retrosplenial cortex, thalamus, and prefrontal cortex (Aggleton 2012). The thalamus in particular holds a privileged position in cortico-subcortical and cortico-cortical bidirectional information flow (Sherman and Guillery 2011). Marked memory deficits follow isolated thalamic damage (Dagenbach et al. 2001; Kubat-Silman et al. 2002; Van der Werf et al. 2003) or electrically induced disruption (Ojemann et al. 1971) in human patients. Experimental lesion studies have identified key contributions of nuclear groups within the thalamus to both long-term (Aggleton and Mishkin 1983; Sziklas and Petrides 1999) and working memory (Isseroff et al. 1982), paralleling dissociated functions of the frontal (Goldman-Rakic 1988) and temporal (Mishkin 1982) cortex with which they are connected. Pertinently, postmortem studies in epileptic patients with hippocampal damage reveal cell loss affecting mediodorsal and lateral thalamic nuclei (Sinjab et al. 2013), now detectable in vivo using advanced brain-imaging approaches (Bernhardt et al. 2012; Keller et al. 2014). Such evidence for thalamic atrophy raises the possibility that, in the context of MTL injury, altered integrity of thalamic nuclei, and disruption of their associated respective thalamo-cortical functional circuits, may contribute to aspects of STM impairment.

Here, we used MRI techniques sensitive to thalamo-cortical connectivity to examine whether altered thalamic integrity impacts on commonly used measures of LTM and STM performance in patients with temporal lobe epilepsy (TLE), selected to have electrophysiological evidence of hippocampal seizures accompanied by normal clinical MRI or hippocampal atrophy. A well-established anatomical connectivity-based approach based on diffusion tensor MRI enabled us to quantify volumes of major thalamic subregions and their relation to hippocampal atrophy. We used a complementary resting fMRI-based functional connectivity approach to correlate neural signals from thalamic subregions with detailed cortical divisions in the prefrontal, temporal, and parietal lobes. Finally, we related anatomical and functional measures of thalamic integrity to standardized clinical measures of LTM and STM function. For this, neuropsychological test scores were used in hierarchical multiple regression models to test the prediction that aberrant extra-MTL thalamo-cortical connectivity contributes to impairments in STM performance in patients with MTL dysfunction. While not informing the nature of computations performed by the hippocampus or thalamus in respect of LTM or STM, our aim was to elucidate potentially differential contributions of dissociated thalamic networks to memory function, as a step towards informing both complex memory systems organization and the potential contribution of extra-hippocampal disruption to STM deficits following hippocampal injury.

Materials and Methods

Participants

Eighteen right-handed patients with TLE aged 31 ± 8.4 years (range 18–49) were recruited through the Oxford Epilepsy Surgery Programme. Patients were selected from a larger cohort to have seizures arising unilaterally from the left MTL based on comprehensive clinical assessment including video-telemetry, high-resolution clinical diagnostic MRI, and neuropsychological evaluation. Clinical MRI revealed reduced hippocampal volumes accompanied by high signal on T_2-weighted sequences, consistent with hippocampal sclerosis (Falconer et al. 1964), in 10 patients. MR imaging was normal or equivocal in 6 patients and revealed subtle MTL focal cortical dysplasia without atrophy in two others. Patients with seizures arising from gross lesions (tumors, cavernoma) were excluded. All patients had drug-resistant seizures (estimated frequency of typical complex partial seizures ranging from 3 to 4 per week to clusters every 2 weeks approximately) and were taking varied combinations of antiepileptic medications (see Table 2). The mean age at onset of chronic seizures was 15.5 ± 9.3 years (range: 2–36) and average duration of epilepsy was 16.5 ± 10.2 years (range 5–42). Controls were 25 right-handed healthy volunteers with no neurological or psychiatric history, age-matched to patients (mean 32.3 ± 6.5 years, range: 20–49, independent

Table 1 Demographic and volumetric data

Measure	Controls, Mean ± SD	Hippocampal atrophy patients, Mean ± SD	Normal hippocampal volume patients, Mean ± SD
Age (years)	32.2 ± 6.5	34.5 ± 7.8	26.6 ± 7.2
Epilepsy onset (years)	—	15.5 ± 10.7	15.5 ± 8
Epilepsy duration (years)	—	19.3 ± 11.3	13 ± 8
Left hippocampus (mm^3)	4027 ± 422	$2515 \pm 332^*$ ($P < 0.001$)	3772 ± 499 (n.s.)
Right hippocampus (mm^3)	4087 ± 365	$3551 \pm 518^*$ ($P = 0.001$)	4126 ± 408 (n.s.)
Left thalamus (mm^3)	$10\,374 \pm 745$	$9141 \pm 1381^*$ ($P = 0.002$)	9930 ± 558 (n.s.)
Right thalamus (mm^3)	9954 ± 643	$8996 \pm 1346^*$ ($P = 0.007$)	9659 ± 647 (n.s.)
Digit span (normalized z-score)	—	9.1 ± 3.5	8.7 ± 3.7
List learning (normalized z-score)	—	-0.76 ± 0.9	-0.79 ± 0.9

Note: Asterisks denote significant volume difference between patients and healthy controls. Hippocampal and thalamic volumes in the normal hippocampal volume patients did not differ from healthy controls.
n.s., not significant.

Table 2 Individual patient data

Patient	Age	Gender	Age at onset	Clinical MRI	Antiepileptic medications	Digit span (normalized z-score)	List learning (normalized z-score)
1	24	F	15	HS	CARB, LEV, PREGAB	10	0.44
2	18	F	9	HS	LAM, CLOB, LEV	6	−0.5
3	40	F	30	FCD	CARB, CLOB	9	−1.42
4	23	F	12	HS	PHEN, LEV, CLOB, LAM	10	0.13
5	42	M	36	HS	LAM, LEV	14	0.39
6	19	F	5	NV	GAB, CLOB, CARB	5	N/A
7	38	M	19	NV	OXCARB, LACOS, CLOB, ACET	7	0.53
8	23	F	2	HS	LEV, OXCARB, ZON	5	−1.23
9	35	F	10	HS	CARB, TOP	6	−0.72
10	24	F	17	NV	LEV, CARB, CLOB	N/A	N/A
11	32	M	22	FCD	CARB, LEV, CLOB	13	−1.83
12	29	F	7	NV	LAC, CLOB, LEV, TOP	6	−1.33
13	30	M	18	NV	LAM, CARB	6	−0.81
14	35	F	18	HS	LAM, LEV	8	−1.42
15	31	M	26	NV	LEV, VAL	16	0.23
16	49	M	7	HS	LAM, GAB	8	−2.09
17	37	M	5	HS	LEV, CARB, CLOB	14	−0.86
18	29	F	21	HS	TOP, LAM, CLOB	9	−1.85

Note: CARB, carbamazepine; LEV, levetiracetam; PREGAB, pregabalin; LAM, lamotrigine; CLOB, clobazam; PHEN, phenytoin; GAB, gabapentin; OXCARB, oxcarbazepine; LAC, lacosamide; ACET, acetazolamide; ZON, zonisamide; TOP, topiramate; VAL, sodium valproate.

samples t-test, $P = 0.58$). Demographic data are presented in Table 1. Informed written consent was obtained from all participants. The study was approved by the South London Research Ethics committee.

Neuropsychology

Each patient had a comprehensive neuropsychological assessment as part of surgical evaluation including tests of general intellectual ability and attentional/executive function from the Wechsler Adult Intelligence Scale (WAIS-IV), and tests of verbal and nonverbal memory abilities from the Brain Injury Rehabilitation Trust Memory and Information Processing Battery (BMIPB). From the WAIS-IV, we selected a composite, age-scaled Digit Span score, integrating performance over forward, backward, and sequence ordering of a list of aurally presented numbers. We chose this composite score rather than simple forward span to capture both temporary maintenance of verbal information as well as active manipulation of the individual digits in memory as an index of working memory function. Additionally, we selected list learning performance from the BMIPB as a measure of LTM acquisition sensitive to MTL integrity (Baxendale et al. 2012). During this task, patients were read a list of 15 unrelated common nouns, then asked to repeat back all items they could recall. This process was repeated a further 5 times with the same list repeated to the patient followed by spontaneous recall. The total number of words recalled over the five trials was converted to normalized z-scores as an index of verbal learning. Digit span was not measured in 1 patient. Two patients were missing verbal learning scores. Individual patient scores are presented in Table 2.

Magnetic Resonance Imaging

MRI data were acquired on a 3T Siemens Verio scanner using a 32-channel head coil. Anatomical T_1-weighted structural images were acquired using a 3D MPRAGE sequence, providing isotropic voxels of $1 \times 1 \times 1$ mm^3. Diffusion MRI datasets were obtained using an echo-planar imaging sequence (TE = 87 ms, TR = 9600 ms, voxel size $2 \times 2 \times 2$ mm^3, 65 slices, GRAPPA acceleration factor = 2) consisting of 8 nondiffusion-weighted and 60 diffusion-weighted images acquired with a b-value of 1000 s $\times$ mm^{-2}. T_2*-weighted blood oxygen level dependent (BOLD) data were acquired during a 5-min resting fMRI scan using an echo-planar imaging sequence (TR = 3.5 s, TE = 30 ms, slice thickness = 2 mm, 54 slices, voxel size $2 \times 2 \times 2$ mm^3). Participants were asked to lie still with their eyes closed but remain awake.

Image Analysis

Subcortical Structural Segmentation: Thalamus and Hippocampus
To determine overall subcortical volumes, the thalamus in each hemisphere was segmented automatically from each participant's T_1-weighted structural image using FMRIB's Integrated Registration and Segmentation Tool (FIRST) (Patenaude et al. 2011). Each segmentation was carefully inspected and manually corrected where necessary to exclude any voxels encroaching on the hippocampus posteriorly or the fornix medially. As hippocampal sclerosis reduces the accuracy of automated segmentation of MTL structures in patients (Pardoe et al. 2009), hippocampi were manually outlined for every participant on their intensity-normalized T_1-weighted structural. Each hippocampus was manually delineated twice in every subject, at least 2 weeks apart, by an experienced rater (N.L.V.), naïve to radiological diagnosis in patients. The intra-class correlation coefficient showed excellent intra-rater reliability for manually defined volumes of both the left (0.96, 95% confidence interval: 0.92–0.98) and right (0.87, 95% confidence interval: 0.77–0.93) hippocampus. Therefore, the first and second hippocampal segmentations were averaged for every subject. Finally, thalamic and hippocampal volumes were normalized for head size by multiplying them with a volumetric scaling factor derived from the automated tool SIENAX as previously described (Menke et al. 2014).

Hippocampal Subdivisions
Increasing evidence supports functional and anatomical divisions within the hippocampus (Aggleton 2012). The relative impact of hippocampal damage on working memory performance may therefore depend on the extent of atrophy affecting subregions of the hippocampus. To divide each person's hippocampus into

anterior and posterior subregions, we used population average masks from our recent study in healthy controls and patients with TLE, some of whom are also included in the present study (Voets et al. 2014). In brief, hippocampal functional divisions were previously identified from resting fMRI data based on preferential patterns of functional connectivity between the hippocampus and cortical regions including the temporal pole, entorhinal cortex, orbitofrontal cortex, posterior parahippocampal gyrus, lingual + fusiform cortex, thalamus, dorsolateral prefrontal cortex, and precuneus + posterior cingulate cortex. Patterns of hippocampo-cortical functional connectivity were summed across patients and healthy controls and thresholded at 50% to create a population average map revealing consistent anterior and posterior hippocampal subregions. Here, we nonlinearly aligned the previously generated population average maps to the T_1-weighted anatomical scan of each individual in the current study to obtain corresponding hippocampus subregion volumes, scaled to each individual's high-resolution brain scan.

Cortical Region-of-Interest Parcellation Using Freesurfer

The multiple nuclear divisions of the thalamus cannot be reliably identified on conventional anatomical MRI scans, but they are dissociable using diffusion-tractography methods sensitive to distinct anatomical connections of thalamic nuclei with large-scale cortical lobes of the brain (Behrens et al. 2003). To identify these thalamic subdivisions in our patients and controls based on anatomical connections with the cortex, we, therefore, first created anatomical masks of the cortical lobes by combining individual cortical parcellations obtained using FreeSurfer (v5.2). Individual subjects' T_1 volumes were linearly aligned to the MNI 305 average brain template, bias corrected, skull-stripped, and segmented into tissue types. The segmented white matter volume was used to derive a surface representing the gray–white matter boundary, which was automatically corrected for topology defects and carefully inspected in each participant for

accurate tissue classification, especially in the anterior temporal lobes. The gray–white surface was inflated to form a sphere and warped to match curvature features across subjects (Dale et al. 1999; Fischl et al. 1999). After alignment to the spherical-space standard curvature template, the cortex was partitioned based on gyral and sulcal structure using an automated segmentation procedure (Desikan et al. 2006). The resulting hemisphere-lateralized cortical parcellations were reformatted and converted into binary masks for compatibility with FMRIB's Software Library.

For diffusion-based classifications, the detailed FreeSurfer-derived cortical parcellations for each individual were combined at the "lobe" level to obtain large-scale cortical masks representing the occipital lobe, temporal lobe, prefrontal cortex, parietal lobe, precentral, and postcentral regions, for each hemisphere separately (Fig. 1a). However, for functional connectivity analyses, each of the detailed FreeSurfer-derived cortical parcellations within the frontal, temporal, and parietal regions were considered separately (see below) for anatomically fine-grained analyses. To restrict resting fMRI partial correlation analyses to regions most likely to be relevant for memory processing, we selected a subset of the detailed cortical Freesurfer parcellations. For the frontal lobe, this included the superior, rostral middle frontal and caudal middle frontal gyri, the medial and lateral orbitofrontal regions, and frontal pole but excluded the 3 Broca's area FreeSurfer parcellations for each hemisphere. For the parietal lobe, we included all four Freesurfer parcels (the superior and inferior parietal lobules, supramarginal gyrus, and precuneus). For the temporal lobe, we selected the superior, middle, inferior temporal, and parahippocampal gyri, the fusiform and entorhinal cortices and the temporal pole, but omitted the "banks of the superior temporal sulcus" and "transverse" parcels (Fig. 1c).

Diffusion-Based Segmentation of the Thalamus

We used a well-characterized diffusion-based classification approach (Behrens et al. 2003) to isolate thalamic subregions in
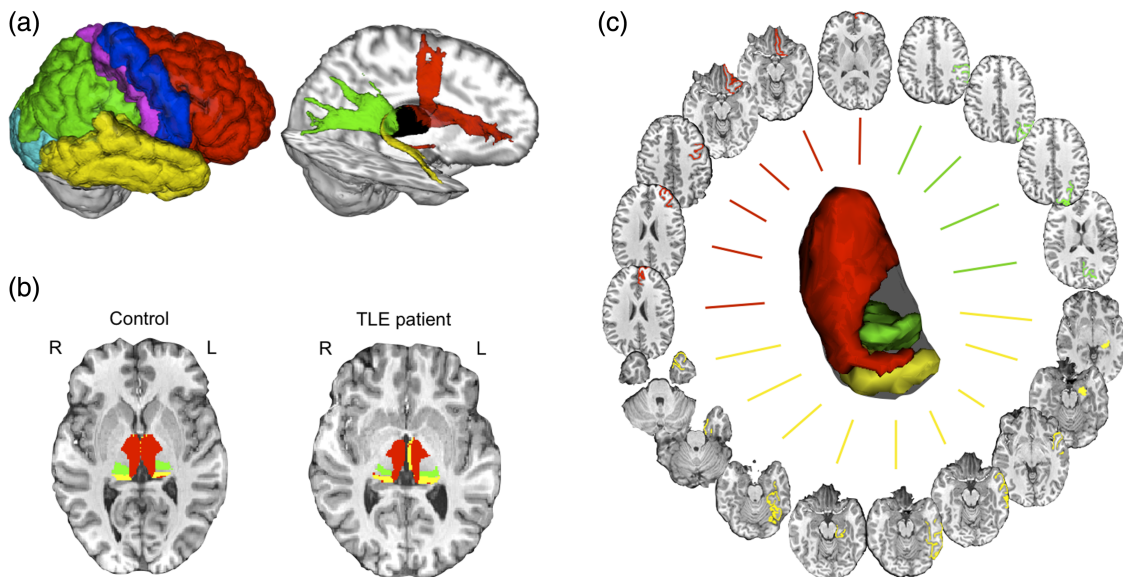

Figure 1. Structural and functional thalamo-cortical connectivity analyses. (*a*) An automated diffusion-based classification approach was used to identify probabilistic anatomical connections between large-scale cortical lobes (top left) and every voxel in the thalamus (thalamus shown in black). This approach segments the thalamus into subregions showing distinct anatomical connectivity profiles (*b*) (red = voxels connected to prefrontal cortex, green = parietal lobe, yellow = temporal lobe) shown in an example healthy control and a patient. (*c*) Resting-state functional MRI signal correlation analysis between the anatomical connectivity-defined parcels of the thalamus (red = voxels connected to prefrontal cortex, green = parietal lobe, yellow = temporal lobe) and detailed FreeSurfer-derived cortical parcellations within each respective lobe, as well anterior and posterior hippocampus subregions from previously generated population maps (Voets et al. 2014). TLE, temporal lobe epilepsy.

each individual. Diffusion data were skull-stripped and affine-registered to the first, nondiffusion-weighted volume to correct for eddy current-induced distortions and head motion. Voxel-wise estimates of fiber orientations (with up to 2 fibers per voxel) and their uncertainty were calculated using FMRIB's Diffusion Toolbox (FDT). The 6 Freesurfer-derived large-scale cortical "lobe" masks were then used in a diffusion-based probabilistic tractography analysis, to classify every voxel in the thalamus according to the cortical "lobe" to which it is preferentially connected (Behrens et al. 2003; Keller et al. 2014). The resulting six classification parcels for each individual were converted into volumes of thalamic regions preferentially connected to each lobe. Thalamic subregion volumes were first scaled by intracranial volume and then converted to ratios (volume of thalamic voxels preferentially connected to a cortical lobe divided by volume of that cortical lobe) to minimize group differences in cortical lobe sizes impacting on structural connectivity.

Functional Connectivity Analysis Between Thalamus Subregions and Cortical Regions of Interests

Next, to quantify functional connectivity (FC) between each of the diffusion-defined segments within the thalamus, and fine-grained cortical regions most likely to be involved in memory function, we measured fMRI signal correlations between the detailed Freesurfer-based subparcellations of the prefrontal, temporal, and parietal lobe and the respective thalamic segments from the diffusion-based classification analysis. Analyses were performed separately for the left and right hemispheres.

Resting fMRI data preprocessing included correction for head motion, correction for geometric distortions at air tissue boundaries using fieldmaps, spatial smoothing using a 5 mm full-width half-maximum Gaussian kernel and high-pass filtering (100 s) to reduce low frequency artefacts. A seed-based correlation approach (SBCA) (O'Reilly et al. 2010) was used to measure thalamo-cortical FC. First, every participant's prefrontal, temporal, and parietal thalamic diffusion-based segments (see Fig. 1b for representative segmentations in a healthy control and TLE patient) were registered to their resting fMRI data using a boundary-based optimized registration method (Greve and Fischl 2009). Next, individuals' detailed FreeSurfer 1 mm pial parcellations (Fig. 1c) were smoothed with a Gaussian filter of 2 mm, registered to their 2 mm fMRI data, and then masked to exclude voxels classified as cerebrospinal fluid (CSF) from automated individual subject tissue segmentations generated using FMRIB's Automated Segmentation Tool (FAST). Finally, 3 SBCAs were performed in each hemisphere.

Resting fMRI signal from each individual's "prefrontal" thalamus segment was correlated with the characteristic time course of each of their 6 prefrontal cortical parcels (superior, rostral middle frontal and caudal middle frontal gyri, medial and lateral orbitofrontal regions and frontal pole). This was repeated, correlating fMRI signal from the thalamic "parietal" segment with that of each of 4 parietal cortical parcels [superior and inferior parietal lobules, supramarginal gyrus and precuneus as defined on the Desikan–Killiany atlas (Desikan et al. 2006)], and finally, from the "temporal" thalamus segment with each of 7 temporal lobe cortical parcels (superior, middle, inferior temporal and parahippocampal gyri, fusiform and entorhinal cortices, temporal pole), as well as the anterior and posterior hippocampus. The time courses representing head motion, CSF, and white matter were regressed out to reduce the influence of structured noise.

Thus, for every participant, we obtained 19 correlation maps in each hemisphere: 9 measuring FC of the "temporal" thalamus segment with each temporal lobe subregion, 6 measuring FC of the "frontal" thalamus segment with each frontal lobe parcel, and 4

measuring FC between the "parietal" thalamic segment and parietal lobe subregions. Each partial correlation map represented, for every voxel in the relevant thalamus segment, its signal correlation magnitude (–1 to 1) with a given cortical subregion in the same hemisphere (accounting for the magnitude of correlation with every other cortical parcel in that lobe). From this, we calculated for every participant the average FC of a given thalamic segment with a respective cortical parcel.

Statistical Analyses

Imaging measures were compared between patients and controls and related to neuropsychological scores using statistical tests implemented in SPSS Statistics (v21). Structural volumetric and diffusion-based measures were compared between groups using multivariate ANCOVAs, co-varying for age. Thalamo-cortical FC from the three thalamic segments in each hemisphere was compared between groups through multivariate ANCOVAs, co-varying for age as well as sizes of the relevant thalamic segment. FC results were Bonferroni-corrected for multiple comparisons separately for each thalamus segment with its corresponding set of correlation maps (9 in each temporal lobe, 6 in each frontal lobe, and 4 in each parietal lobe). Relationships between behavioral and imaging measures in patients were established first using 2-tailed Pearson's partial correlations, removing variability associated with age. Subsequently, brain-imaging measures associated with STM performance were entered into a hierarchical linear regression model to assess their unique predictive contribution to performance variability in this memory domain.

Results

Global Thalamus Volumes

Multivariate ANCOVAs revealed a significant effect of group on overall thalamus sizes. Relative to healthy controls, TLE patients had smaller thalamic volumes, both in the ipsilateral left ($F = 9.55$, $P = 0.004$) and contralateral right hemisphere ($F = 6.15$, $P = 0.017$) (Fig. 2b). Across patients and controls, as well as within each subgroup, hippocampal volume correlated with thalamus volume in both hemispheres (left hemisphere: $R = 0.58$, $P < 0.001$; right hemisphere: $R = 0.54$, $P < 0.001$) (Fig. 2c). Duration of epilepsy did not correlate with either thalamic or hippocampal volumes ($P > 0.1$).

Volumes of Connectivity-Defined Thalamus Subregions

Multivariate ANCOVAs revealed an effect of group also on "ipsilateral," but not contralateral, thalamic subregional volumes for TLE patients compared with controls ($F = 3.51$, $P = 0.024$). This was due to a significant reduction in thalamic voxels preferentially connected to the parietal lobe in the epileptic (left) hemisphere ($F = 6.40$, $P = 0.015$) (Fig. 3b). There was no difference between patients and controls in thalamo-prefrontal or thalamo-temporal volume ratios.

Thalamo-Cortical FC

The TLE patient group showed abnormally increased FC relative to controls between the contralateral (right) but not the ipsilateral (left) thalamic "parietal segment" and precuneus after Bonferroni-correction for four parietal cortical parcels ($F = 7.52$, corrected to $P = 0.036$). However, there was no significant difference between the patients and controls in FC between the thalamus diffusion-defined prefrontal segment and any cortical subregions within the prefrontal lobe, either ipsi- or contralaterally.
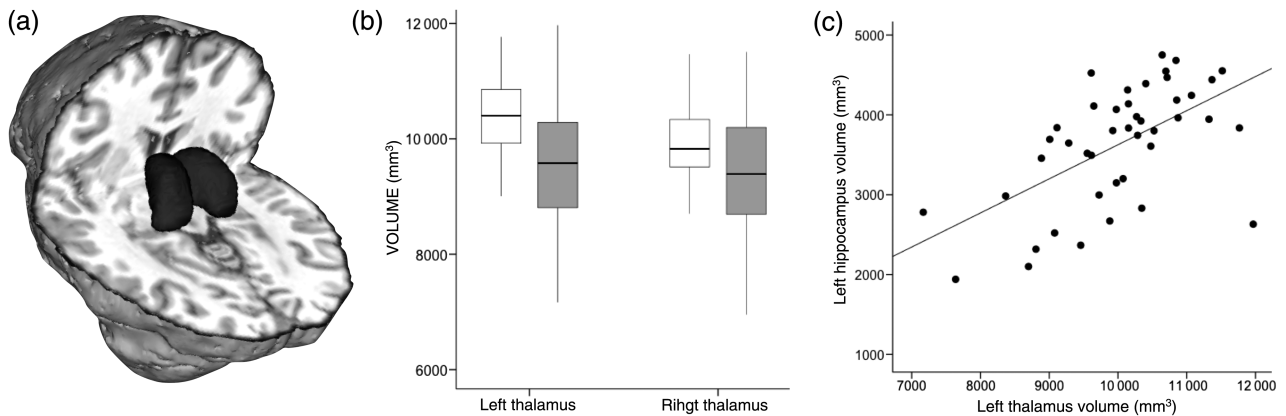
Figure 2. Global thalamic volumes in epilepsy and relation to hippocampal atrophy. (*a*) Example automated segmentation of the thalamus in a representative healthy control. (*b*) Overall thalamus volumes were reduced in TLE patients (light grey bars) relative to healthy controls (white bars) (boxplots depict mean [± 2 standard deviations]) in both hemispheres. (*c*) Hippocampal and thalamus volumes were significantly correlated in all subjects ($R = 0.58$, $P < 0.001$).

Similarly, FC between the thalamus "temporal segment" and temporal lobe subregions in patients remained within the normal range.

Impact on Neuropsychological Performance

To determine the extent to which observed changes in thalamic volumes and connection patterns impacted on memory integrity in TLE patients, we first explored associations between our structural and functional MRI measures and neuropsychological performance on test of STM and LTM. Seven patients achieved composite digit span scores of 7 or less (mean score for TLE group: 8.94 ± 3.5, range: 5 to 16), while 5 patients had list learning score that fell in the borderline/impaired range (z-scores of −1.34 or lower; mean for TLE group: −0.77 ± 0.89, range 0.53 to −2.09). Neither duration of epilepsy nor age at onset of habitual seizures correlated significantly with either neuropsychological test measure.

STM (composite digit span) performance in patients was not significantly correlated with global hippocampal volumes. However, smaller volumes of the posterior ipsilateral hippocampus were associated with poorer digit span ($R = 0.55$, $P = 0.027$). Neither global nor subregional thalamus volumes correlated with digit span. Instead, lower digit span in patients was associated with measures of both thalamo-prefrontal and thalamo-parietal FC. Specifically, lower FC between the contralateral thalamic prefrontal segment and caudal middle frontal gyrus ($R = 0.70$, $P = 0.003$) (Fig. 4a) was associated with lower digit span; this was also a trend ipsilaterally ($R = 0.46$, $P = 0.075$). Similarly, lower FC between the contralateral thalamic "parietal segment" and the supramarginal gyrus reflected lower digit span performance ($R = 0.53$, $P = 0.034$).

In contrast to these STM associations with thalamo-prefrontal and thalamo-parietal FC, LTM performance reflected thalamo-temporal FC. Lower list learning performance was seen in patients with lower ipsilateral thalamo-entorhinal FC ($R = 0.57$, $P = 0.028$) (Fig. 4b). In addition, list learning was negatively correlated with volume ratios of the thalamic "prefrontal segment" both ipsi- ($R = −0.67$, $P = 0.006$) and contralaterally ($R = −0.72$, $P = 0.002$) in patients. However, this was not reflected in accompanying associations between list learning performance and either thalamo-prefrontal or thalamo-parietal FC.

Finally, to directly assess the specificity of this apparent dissociation in thalamo-cortical pathways associated with STM, we performed a hierarchical multiple regression analysis. For this analysis, we included age in the first step of the multiple

regression, and in the second step, we modeled the unique predictive value of each measure associated with digit span (from the analysis above), to identify the magnitude and order in which each contribute to STM performance. We also included thalamo-entorhinal resting connectivity (found to correlate with list learning), to help interpret the specificity of our correlation findings. This model as a whole was a significant predictor of STM performance, accounting for 86% of variance in digit span ($F = 10.2$, $P = 0.001$). Age explained 10.4% variance in digit span performance. When controlling for age, our imaging measures accounted for an additional 75.6% variance (significant F change: 0.001). Of the individual variables, volume of the posterior ipsilateral hippocampus ($\beta = 0.47$, $P = 0.007$) and FC between the contralateral thalamus and caudal middle frontal gyrus ($\beta = 0.99$, $P = 0.013$) made significant unique contributions to the model. Ipsilateral thalamo-caudal middle frontal ($P = 0.09$), contralateral thalamo-supramarginal ($P = 0.16$), and, importantly, ipsilateral thalamo-entorhinal ($P = 0.26$) resting FC did not contribute significantly to digit span performance. Removing ipsilateral thalamo-caudal middle frontal connectivity (correlated with contralateral thalamo-caudal middle frontal connectivity) from the model did not significantly impact these findings.

Finally, we repeated the hierarchical linear regression analysis, controlling for age and modeling each of the measures associated with list learning to identify the most significant predictors of LTM performance. As above, we included in the LTM model also those variables correlated with digit span, to assess the specificity of thalamo-cortical measures for both memory domains. The model as a whole was a significant predictor of LTM performance ($F = 5.16$, $P = 0.022$), explaining 92.5% of variance in list learning. Age explained 22.9% variance in list learning performance. After controlling for age, the neural measures explained an additional 80.2% variance (significant F change = 0.019). Of the individual measures, only ipsilateral thalamo-entorhinal cortex resting connectivity contributed significantly to list learning performance ($\beta = 0.72$, $P = 0.049$). Neither ipsilateral nor contralateral thalamic–prefrontal connectivity volume ratios, nor any of the measures correlated with digit span performance, reached significance as predictors of list learning in this model.

Effect of Hippocampal Atrophy on Thalamo-Cortical Interaction

Both secondary deafferentation of thalamic connections from an atrophic hippocampus and propagation of epileptic activity could
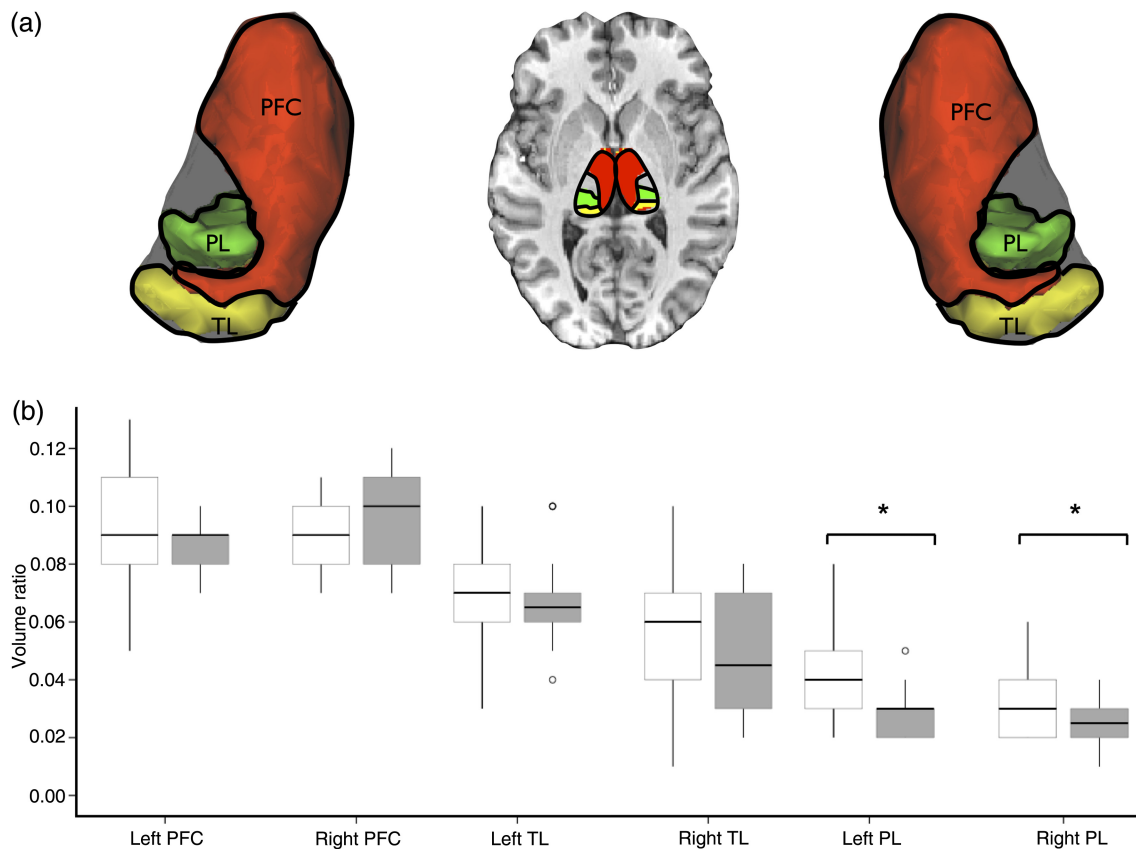
Figure 3. Anatomical connectivity of the thalamus in temporal lobe epilepsy. (*a*) Volume ratios were calculated of tractography-defined voxels within the thalamus showing preferential anatomical connections with the temporal lobe (yellow), frontal lobe (red), and parietal lobe (green). (*b*) Asterisks denote significant reductions specifically in anatomical connections between the thalamus and parietal lobe in patients relative to controls ($P < 0.05$), that was driven by the subgroup of patients with hippocampal atrophy. Boxplots depict volume ratios (± 2 standard deviations) of thalamic connectivity-defined regions in controls (white bars) and patients with TLE (gray bars). TLE, temporal lobe epilepsy; PFC, prefrontal cortex; TL, temporal lobe; PL, parietal lobe.

in theory contribute to functional thalamic disruption in TLE (Sinjab et al. 2013). If thalamo-cortical dysfunction reflects the thalamus' role in propagation of epileptic activity, similar patterns of disruption might be expected across all patients with chronic TLE, regardless of the size of the hippocampus. Conversely, if hippocampal sclerosis compounds thalamic atrophy, greater thalamo-cortical disruption would be expected in patients with smaller hippocampal volumes. To investigate these possibilities, we performed a preliminary analysis, dividing our patients into 2 groups: Those with ipsilateral hippocampal volumes 2 standard deviations or more below the range of our healthy controls ("atrophy" group, $n = 10$) and those with ipsilateral hippocampal volumes within the normal range ($n = 8$).

Despite the reduced sample sizes, patients with hippocampal atrophy—but not those with normal hippocampal volumes—showed bilateral reductions in global thalamic volumes (left: $F = 10.91$, $P = 0.002$; right: $F = 7.73$, $P = 0.009$) (Fig. 2*c*), as well as in volume ratios of connections with the ipsilateral parietal lobe ($F = 4.34$, $P = 0.045$).

Patients with and without hippocampal atrophy showed correspondingly divergent associations between thalamo-cortical communication and digit span. In normal volume patients, digit span performance correlated bilaterally with both thalamo-caudal middle frontal FC (right hemisphere: $R = 0.792$, $P = 0.034$, left hemisphere: $R = 0.788$, $P = 0.036$) and thalamo-supramargical FC (right hemisphere: $R = 0.915$, $P = 0.004$, left hemisphere: $R = 0.742$, $P = 0.056$).

Conversely, in patients with left hippocampal volume loss, only FC between the contralateral (right) thalamus and caudal middle frontal gyrus remained significantly correlated with digit span ($R = 0.744$, $P = 0.014$). The loss of ipsilateral thalamo-prefrontal FC association with digit span may reflect aberrant, heightened thalamo-caudal middle frontal gyrus FC seen in the affected (left) hemisphere ($F = 4.04$, $P = 0.053$, corrected for thalamic prefrontal segment volume) of patients with hippocampal atrophy, but not patients with normal volumes, relative to controls.

We did not contrast list learning between the patient subgroups as both patients missing these values were from the smaller normal volume group. We did not repeat hierarchical multiple regression analyses based on the reduced sample size in these subgroups.

Discussion

Deficits in amnestic patients on some tests of STM (Nichols et al. 2006; Olson, Page, et al. 2006; Hartley et al. 2007; Pertzov et al. 2013), but not others (Drachman and Arbit 1966; Zarahn et al. 2005; Jeneson et al. 2010; Baddeley et al. 2011), have sparked debate about a potentially direct role for the hippocampus in STM (Cashdollar et al. 2011). Here, we tested an alternative possibility that deficits on aspects of STM reflect disruption of thalamo-cortical communication associated with MTL damage. Multimodal MRI was used to quantify thalamo-cortical connectivity in
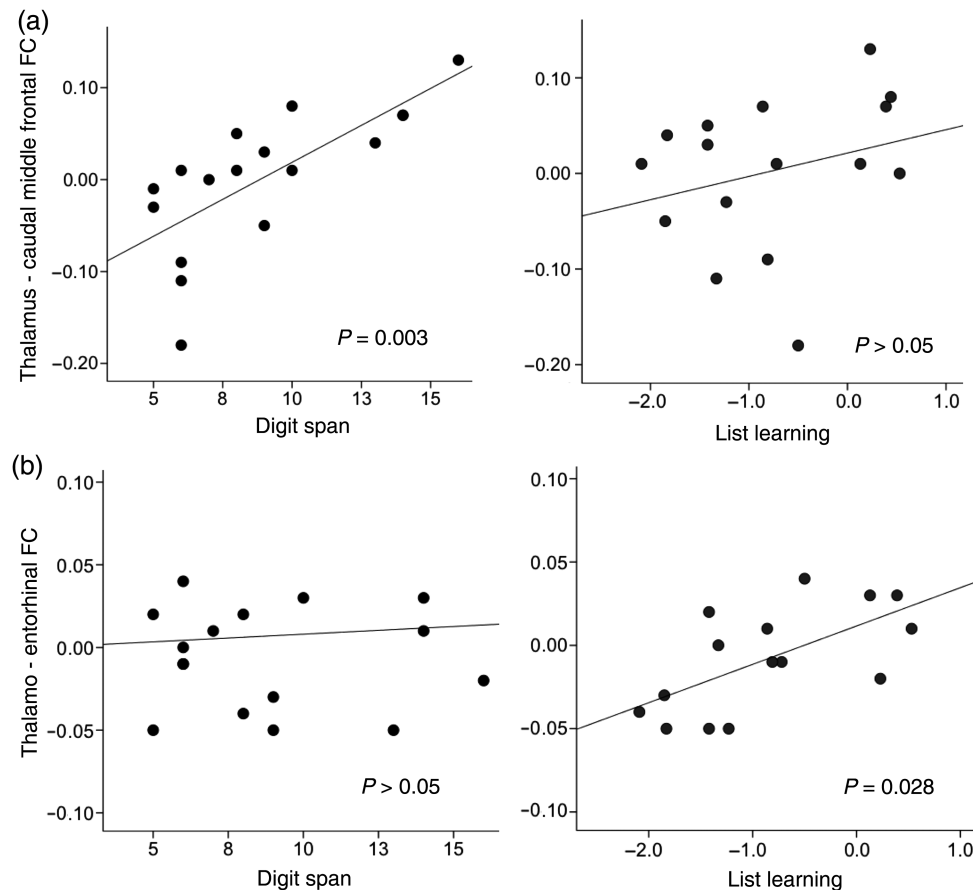
Figure 4. Association between thalamo-cortical connectivity and STM and LTM performance. (*a*) In patients, thalamo-prefrontal FC (with the caudal middle frontal gyrus) correlated with measures of STM ($R = 0.70$, $P = 0.003$) but not list learning. (*b*) Conversely, thalamo-temporal FC (with the entorhinal cortex) correlated with LTM ($R = 0.57$, $P = 0.028$) but not STM performance. FC, functional connectivity.

patients with epilepsy arising from the left MTL, with and without measurable hippocampal atrophy. Resting-state FC analyses revealed a unique contribution of extra-MTL thalamo-cortical pathways to STM performance. Furthermore, thalamic microstructure and cortical FC reflected magnitudes of MTL damage in patients, with the greatest thalamic structural and functional disruption seen in patients with abnormally reduced hippocampal volumes. These results provide evidence that thalamo-cortical disruption might contribute to STM impairments in MTL-damaged patients.

It is increasingly recognized that thalamic nuclei do not simply relay information, but actively contribute to cognitive processes in ways consistent with—though perhaps qualitatively distinct from—their associated neocortical areas (Hunt and Aggleton 1991; de Bourbon-Teles et al. 2014). Although the role of thalamic nuclei in memory processes remains incompletely understood, lesion and electrophysiological data suggest that LTM symptoms most commonly arise after anterior thalamic nucleus damage, while STM deficits may involve ventral mediodorsal, midline, and ventral anterior structures (Van der Werf et al. 2003). Verbal STM deficits have also been elicited with electrical stimulation of the left pulvinar nucleus (Ojemann and Fedio 1968) and ventrolateral sites (Ojemann et al. 1971), lesions to which produce deficits of visual attention orientation (de Bourbon-Teles et al. 2014).

Thalamic contributions to memory are thought to reflect partially independent routes of information flow between thalamic subregions and functionally distinct neocortical areas (Bentivoglio et al. 1997). Within the mediodorsal nucleus, regarded as the prefrontal cortex "gateway" (Tanibuchi and Goldman-Rakic 2003), anatomical connections point to at least 3 neural circuits potentially supporting memory processing in primates (Mitchell and Chakraborty 2013). These include a medial system interconnected with orbitofrontal and ventromedial prefrontal cortex as well as MTL structures; a central system preferentially connected with the dorsolateral prefrontal cortex (but not with the MTL); and a lateral system consisting of intralaminar nuclei with diffuse prefrontal, anterior cingulate, and basal ganglia projections. Conversely, the anterior thalamic nuclei form a separate circuit interconnected with the hippocampal formation, mammillary bodies, anterior cingulate, and retrosplenial cortex (Aggleton et al. 2010). Finally, lateral posterior nuclei, including the "association" pulvinar complex, show extensive connections including with prefrontal, posterior parietal, and limbic regions (Romanski et al. 1997). Differential disruption to these parallel thalamo-cortical pathways would therefore be predicted to explain variability in the nature and extent of memory deficits.

Consistent with this prediction, in our study, STM and LTM deficits reflected FC within distinct thalamo-cortical networks. Lower digit span performance in patients was associated with lower resting-state fMRI signal correlations between the regions within the thalamus preferentially connected to the prefrontal cortex (based on anatomical connectivity) and the caudal middle

frontal gyri. Tract tracing studies in nonhuman primates indicate preferential connections from the central mediodorsal region to this cortical area (Mitchell and Chakraborty 2013), which has been attributed a specific role in ordering information in STM (Henson et al. 2000).

In contrast, impaired list learning performance reflected FC between the entorhinal cortex and the connectivity-defined thalamic "temporal" segment, grossly corresponding to the anterior nucleus and parts of the medial mediodorsal nucleus anatomically interconnected with the MTL. The entorhinal cortex constitutes the major communication route of the hippocampus and has been shown to both interact with the hippocampus during (Igarashi et al. 2014) and independently contribute to (Gaskin and White 2013; Yang et al. 2014) aspects of learning.

These findings support fMRI and electrophysiological data demonstrating key roles for thalamo-cortical communication in STM processing. Working memory load-related neural activity in dorsolateral prefrontal and parietal cortices is also seen in the thalamus using fMRI (Callicott et al. 1999). Electrophysiological recordings further demonstrate coordinated prefrontal, parietal, and thalamic neuronal firing during task delay periods in nonhuman primates (Fuster and Alexander 1971; Tanibuchi and Goldman-Rakic 2003), disruption of which induces working memory deficits in rodents (Parnaudeau et al. 2013).

Interestingly, digit span reflected contralateral, right hemisphere thalamo-cortical FC, while list learning was predicted by ipsilateral, left hemisphere thalamo-temporal FC. The most parsimonious explanation for this hemispheric dissociation is that lateralized left temporal lobe damage is known to produce deficits in verbal learning and LTM (Milner 1971). Our finding of reduced list learning with reduced left thalamo-entorhinal FC is consistent with longitudinal observations showing that magnitudes of verbal LTM loss reflect extents of functional left MTL tissue damage (Powell et al. 2008). Conversely, imaging studies often reveal bilateral fronto-parietal activity during tasks involving STM, thought to reflect stimulus-independent complex processing demands (Nystrom et al. 2000; Wager and Smith 2003; Chein et al. 2011) within widely distributed circuits subserving working memory (Goldman-Rakic 1988). We therefore speculate that in the context of unilateral disruption to bilaterally represented STM networks, patients may rely on remaining (perhaps less efficient) thalamo-cortical connections in the unaffected hemisphere.

This interpretation is supported by disrupted anatomical and functional thalamo-cortical connectivity observed in patients with—but not without—hippocampal atrophy. We found that hippocampal atrophy patients showed fewer parietal lobe connections and abnormally elevated thalamo-prefrontal FC in the epileptic hemisphere. Concurrently, hippocampal atrophy patients showed a loss of functional correlations with STM within the corresponding networks. Indeed, while in hippocampus-intact patients, digit span reflected bilateral thalamo-prefrontal and thalamo-parietal FC, in hippocampal-atrophy patients, digit span performance correlated only with contralateral thalamo-prefrontal communication. A loss of parietal anatomical connections could possibly disrupt functional associations reliant on communication between medial pulvinar/lateral dorsal and supramarginal neurons reportedly involved in phonological storage (Henson et al. 2000) and number manipulations (Price et al. 2013). The lack of indication for abnormal thalamo-supramarginal FC in patients implies potentially independent contributions of these thalamic nuclei to aspects of verbal STM (Ojemann and Fedio 1968). Additionally, hippocampal atrophy patients showed abnormally heightened FC between the thalamus and caudal

middle frontal gyrus in the epileptic hemisphere, which no longer correlated with digit span. Although the mechanism for this FC disruption is unclear, these results mirror selective limbic fiber degeneration seen in patients with—but not without—hippocampal sclerosis, especially along the fornix (Concha et al. 2009) which connects the hippocampus with the thalamus and mammillary bodies (Aggleton et al. 1986).

What about the role of the hippocampus in STM? This study was not specifically designed to disentangle mnemonic computations performed by the hippocampus (or indeed the thalamus), but some findings might be pertinent. Although global hippocampus volumes were not related to digit performance, smaller volume of specifically the *posterior* epileptic hippocampus correlated with and uniquely predicted variance in digit span performance. This region is considered to form part of a posterior memory network composed of the retrosplenial cortex, dorsolateral prefrontal cortex, and posterior sensory cortices, in contrast to an anterior hippocampal memory network including the amygdala, orbitofrontal cortex, and temporal pole (Aggleton 2012). However, the association between digit span and posterior hippocampal volumes does not allow us to dissociate the role of direct connections to dorsolateral prefrontal cortex via the cingulum or fronto-occipital fasciculus (Goldman-Rakic et al. 1984) from indirect thalamo-cortical projections via the fornix, since chronic epilepsy patients show structural damage along the entire limbic circuit (Focke et al. 2008).

Which experimental task demands/manipulations unveil a memory deficit across short delay intervals in patients with hippocampal lesions remains actively debated. While many tasks have focused on relational binding, deficits in associative memory are not the only reported findings. For example, impairments have also been identified for faces (Nichols et al. 2006; Olson, Moore, et al. 2006). Conversely, not all associative tasks are impaired in MTL-damaged patients. Simple associative memory performance appears intact when trials involve a small number of associations, with impairments emerging only on larger set sizes (Jeneson et al. 2010; Pertzov et al. 2013). These findings echo early observations of markedly reduced general storage capacity in patients with hippocampal lesions on an extended digit span task, most pronounced on digit set sizes exceeding 6 (Drachman and Arbit 1966).

An alternative conceptual framework to associative/non-associative processing for these previously observed STM deficits is the level to which stimulus computations exceed the span of immediate/STM and begin to call upon LTM "supraspan" resources (Yonelinas 2013). Drachman and Arbit already in 1966 proposed that complex information, including difficult item associations but perhaps also feature-dependent stimuli such as faces (Nichols et al. 2006), may rely on LTM stores – just like supraspan information – depending on how many item/information features can be held in immediate memory (Drachman and Arbit 1966). Consequently, it has been proposed that instead of the MTL being critically involved in certain types of STM, some types of task call upon LTM processes (Jeneson and Squire 2012). This distinction might potentially explain conflicting neuroimaging findings of hippocampal activity during the delay period for novel face (Ranganath and D'Esposito 2001) but not letter (Zarahn et al. 2005) stimuli.

Our results lend support to the notion that thalamic nuclei may pivotally contribute to deficient STM performance in patients with MTL damage, perhaps by mediating complex computational demands between immediate and long-term stores (Vertes et al. 2007). Thalamic neurons contribute to information processing and gating (Fuster and Alexander 1971; Vertes et al. 2007; Rotshtein et al. 2011) as well as associative learning

([Winocur 1985](#); [Hunt and Aggleton 1991](#); [Gibb et al. 2006](#)), see [Mitchell and Chakraborty 2013](#) for a review), and perhaps stimulus maintenance or selection ([Parnaudeau et al. 2013](#)) in animals, and have been shown to modulate neocortical synchrony based on attentional demands, at least in the visual domain, consistent with a putative role in cortical information distribution ([Saalmann et al. 2012](#)).

In humans, recent fMRI evidence shows differential thalamic nuclei activate during learning and retrieval phases on associative learning tasks in healthy volunteers ([Pergola et al. 2013](#)), while relational memory deficits are reported in patients with certain thalamic lesions ([Soei et al. 2008](#)). Further studies are clearly needed to refine categories of computations and/or stimulus features fundamentally reliant on the hippocampus, how processing demands alter the requirements for STM versus LTM, and the extent to which this balance may hinge upon thalamic modulation of activity within wider neural networks supporting memory function. In this respect, patients with focal thalamic lesions might provide additional unique insight into consequences of lesions disrupting distinct thalamo-cortical memory networks on hippocampal processes.

Although our correlational and regression results support independent contributions of specific thalamo-prefrontal cortex pathway disruption to STM deficits, such evidence does not, of course, inform causal directions or the etiology of thalamo-cortical disruption. Secondary degeneration following hippocampal atrophy should preferentially affect the anterior thalamic nucleus, whereas postmortem ([Sinjab et al. 2013](#)) and imaging data ([Barron et al. 2012](#); [Bernhardt et al. 2012](#); [Duzel et al. 2006](#)) identify primarily mediodorsal, pulvinar, and lateral nuclear damage. Since midline thalamic nuclei have been implicated in seizure spread in animal models of temporal lobe ([Bertram et al. 2001](#)), but also generalized, epilepsy ([Avoli and Gloor 1982](#)), hippocampal atrophy alone may not fully account for thalamo-cortical disruption in our patients. Furthermore, subtle damage in our normal volume subgroup cannot be excluded without histopathology. Longitudinal and developmental studies will be necessary to shed further light onto the mechanisms associated with thalamic dysfunction in this epileptic model of MTL damage.

We defined hippocampal atrophy as volumes falling 2 standard deviations below those of age-matched controls. To determine the influence of this classification, we repeated our patient subgroup analyses with a more liberal cutoff of hippocampal volumes <1.5 SD from those of controls. According to this revised classification, 1 patient was reclassified to the "atrophic" group. Aside from slightly reduced statistical significance for correlations between imaging markers and digit span performance in the downsized "normal range" group, defining atrophy using a 1.5 SD cutoff did not alter the overall pattern of findings in the subgroup comparisons.

Certain uncontrollable clinical variables potentially contribute to our findings. All patients were taking different combinations of antiepileptic drugs. The extent to which these influence fMRI signals is not known and could not be assessed in our modest sample size. Additionally, some antiepileptic medications affect levels of motivation, arousal, and/or attention that could impact on cognitive performance, although their exact mechanism of action remains poorly understood. It seems unlikely that medication alone selectively influenced thalamo-temporal versus thalamo-prefrontal circuits in a way that might produce the dissociated anatomical-behavioral relationships we observed, especially given the range of drugs and doses taken by patients in this cohort.

In conclusion, patients with epilepsy-related MTL dysfunction show thalamic atrophy co-varying with extents of hippocampal damage. Pathological extents of individual subcortical structures alone are not sensitive markers of performance, highlighting the importance of widespread functional circuits to STM and LTM. Extending previous reports linking global thalamic volumes with memory deficits in patients with MTL dysfunction ([Seidenberg et al. 2008](#); [Stewart et al. 2009](#)), these findings demonstrate that spatially distinct thalamo-cortical functional networks are associated with STM and LTM deficits and are specifically affected in patients with hippocampal atrophy rather than those with preserved hippocampal volumes. We propose that beyond the direct impact of MTL lesions, associated effects on specific thalamo-cortical circuits might play an important role in the etiology of STM deficits and may aid to reconcile previous disparate findings in MTL-damaged patients.

Funding

Notes

References

Aggleton JP. 2012. Multiple anatomical systems embedded within the primate medial temporal lobe: implications for hippocampal function. Neurosci Biobehav Rev. 36(7):1579–1596.

Aggleton JP, Desimone R, Mishkin M. 1986. The origin, course, and termination of the hippocampothalamic projections in the macaque. J Comp Neurol. 243(3):409–421.

Aggleton JP, Mishkin M. 1983. Memory impairments following restricted medial thalamic lesions in monkeys. Exp Brain Res. 52(2):199–209.

Aggleton JP, O'Mara SM, Vann SD, Wright NF, Tsanov M, Erichsen JT. 2010. Hippocampal-anterior thalamic pathways for memory: uncovering a network of direct and indirect actions. Eur J Neurosci. 31(12):2292–2307.

Alvarez P, Zola-Morgan S, Squire LR. 1994. The animal model of human amnesia: long-term memory impaired and short-term memory intact. Proc Natl Acad Sci USA. 91(12):5637–5641.

Avoli M, Gloor P. 1982. Interaction of cortex and thalamus in spike and wave discharges of feline generalized penicillin epilepsy. Exp Neurol. 76(1):196–217.

Baddeley A, Allen R, Vargha-Khadem F. 2010. Is the hippocampus necessary for visual and verbal binding in working memory? Neuropsychologia. 48(4):1089–1095.

Baddeley A, Jarrold C, Vargha-Khadem F. 2011. Working memory and the hippocampus. J Cogn Neurosci. 23(12):3855–3861.

Barron DS, Fox PM, Laird AR, Robinson JL, Fox PT. 2012. Thalamic medial dorsal nucleus atrophy in medial temporal lobe epilepsy: a VBM meta-analysis. Neuroimage Clin. 2:25–32.

Baxendale S, Thompson PJ, Duncan JS. 2012. Neuropsychological function in patients who have had epilepsy surgery: a long-term follow-up. Epilepsy Behav. 23(1):24–29.

Behrens TE, Johansen-Berg H, Woolrich MW, Smith SM, Wheeler-Kingshott CA, Boulby PA, Barker GJ, Sillery EL, Sheehan K, Ciccarelli O, et al. 2003. Non-invasive mapping of connections

between human thalamus and cortex using diffusion imaging. Nat Neurosci. 6(7):750–757.

Bentivoglio M, Aggleton JP, Mishkin M. 1997. The thalamus and memory formation. In: Steriade M, Jones EJ, editors. Thalamus, Vol. 2: experimental and clinical aspects. Amsterdam: Elsevier. p. 689–721.

Bernhardt BC, Bernasconi N, Kim H, Bernasconi A. 2012. Mapping thalamocortical network pathology in temporal lobe epilepsy. Neurology. 78(2):129–136.

Bertram EH, Mangan PS, Zhang D, Scott CA, Williamson JM. 2001. The midline thalamus: alterations and a potential role in limbic epilepsy. Epilepsia. 42(8):967–978.

Callicott JH, Mattay VS, Bertolino A, Finn K, Coppola R, Frank JA, Goldberg TE, Weinberger DR. 1999. Physiological characteristics of capacity constraints in working memory as revealed by functional MRI. Cereb Cortex. 9(1):20–26.

Cashdollar N, Duncan JS, Duzel E. 2011. Challenging the classical distinction between long-term and short-term memory: reconsidering the role of the hippocampus. Future Neurol. 6 (3):351–362.

Chein JM, Moore AB, Conway AR. 2011. Domain-general mechanisms of complex working memory span. Neuroimage. 54(1): 550–559.

Concha L, Beaulieu C, Collins DL, Gross DW. 2009. White-matter diffusion abnormalities in temporal-lobe epilepsy with and without mesial temporal sclerosis. J Neurol Neurosurg Psychiatry. 80(3):312–319.

Corkin S. 1984. Lasting consequences of bilateral medial temporal lobectomy - clinical course and experimental findings in Hm. Seminars Neurol. 4(2):249–259.

Dagenbach D, Kubat-Silman AK, Absher JR. 2001. Human verbal working memory impairments associated with thalamic damage. Int J Neurosci. 111(1–2):67–87.

Dale AM, Fischl B, Sereno MI. 1999. Cortical surface-based analysis. I. Segmentation and surface reconstruction. Neuroimage. 9(2):179–194.

de Bourbon-Teles J, Bentley P, Koshino S, Shah K, Dutta A, Malhotra P, Egner T, Husain M, Soto D. 2014. Thalamic control of human attention driven by memory and learning. Curr Biol. 24(9):993–999.

Desikan RS, Segonne F, Fischl B, Quinn BT, Dickerson BC, Blacker D, Buckner RL, Dale AM, Maguire RP, Hyman BT, et al. 2006. An automated labeling system for subdividing the human cerebral cortex on MRI scans into gyral based regions of interest. Neuroimage. 31(3):968–980.

Drachman DA, Arbit J. 1966. Memory and the hippocampal complex. II. Is memory a multiple process? Arch Neurol. 15 (1):52–61.

Duzel E, Schiltz K, Solbach T, Peschel T, Baldeweg T, Kaufmann J, Szentkuti A, Heinze HJ. 2006. Hippocampal atrophy in temporal lobe epilepsy is correlated with limbic systems atrophy. J Neurol. 253(3):294–300.

Falconer MA, Serafetinides EA, Corsellis JA. 1964. Etiology and pathogenesis of temporal lobe epilepsy. Arch Neurol. 10:233–248.

Fischl B, Sereno MI, Dale AM. 1999. Cortical surface-based analysis. II: Inflation, flattening, and a surface-based coordinate system. Neuroimage. 9(2):195–207.

Focke NK, Yogarajah M, Bonelli SB, Bartlett PA, Symms MR, Duncan JS. 2008. Voxel-based diffusion tensor imaging in patients with mesial temporal lobe epilepsy and hippocampal sclerosis. Neuroimage. 40(2):728–737.

Fuster JM, Alexander GE. 1971. Neuron activity related to short-term memory. Science. 173(3997):652–654.

Gaskin S, White NM. 2013. Parallel processing of information about location in the amygdala, entorhinal cortex and hippocampus. Hippocampus. 23(11):1075–1083.

Gibb SJ, Wolff M, Dalrymple-Alford JC. 2006. Odour-place paired-associate learning and limbic thalamus: comparison of anterior, lateral and medial thalamic lesions. Behav Brain Res. 172 (1):155–168.

Goldman-Rakic PS. 1988. Topography of cognition: parallel distributed networks in primate association cortex. Annu Rev Neurosci. 11:137–156.

Goldman-Rakic PS, Selemon LD, Schwartz ML. 1984. Dual pathways connecting the dorsolateral prefrontal cortex with the hippocampal formation and parahippocampal cortex in the rhesus monkey. Neuroscience. 12(3):719–743.

Greve DN, Fischl B. 2009. Accurate and robust brain image alignment using boundary-based registration. Neuroimage. 48(1):63–72.

Hartley T, Bird CM, Chan D, Cipolotti L, Husain M, Vargha-Khadem F, Burgess N. 2007. The hippocampus is required for short-term topographical memory in humans. Hippocampus. 17(1):34–48.

Henson RN, Burgess N, Frith CD. 2000. Recoding, storage, rehearsal and grouping in verbal short-term memory: an fMRI study. Neuropsychologia. 38(4):426–440.

Hunt PR, Aggleton JP. 1991. Medial dorsal thalamic lesions and working memory in the rat. Behav Neural Biol. 55(2):227–246.

Igarashi KM, Lu L, Colgin LL, Moser MB, Moser EI. 2014. Coordination of entorhinal-hippocampal ensemble activity during associative learning. Nature. 510(7503):143–147.

Isseroff A, Rosvold HE, Galkin TW, Goldman-Rakic PS. 1982. Spatial memory impairments following damage to the mediodorsal nucleus of the thalamus in rhesus monkeys. Brain Res. 232(1):97–113.

Jeneson A, Mauldin KN, Squire LR. 2010. Intact working memory for relational information after medial temporal lobe damage. J Neurosci. 30(41):13624–13629.

Jeneson A, Squire LR. 2012. Working memory, long-term memory, and medial temporal lobe function. Learn Mem. 19(1):15–25.

Keller SS, O'Muircheartaigh J, Traynor C, Towgood K, Barker GJ, Richardson MP. 2014. Thalamotemporal impairment in temporal lobe epilepsy: a combined MRI analysis of structure, integrity, and connectivity. Epilepsia. 55(2):306–315.

Kubat-Silman AK, Dagenbach D, Absher JR. 2002. Patterns of impaired verbal, spatial, and object working memory after thalamic lesions. Brain Cogn. 50(2):178–193.

Menke RA, Szewczyk-Krolikowski K, Jbabdi S, Jenkinson M, Talbot K, Mackay CE, Hu M. 2014. Comprehensive morphometry of subcortical grey matter structures in early-stage Parkinson's disease. Hum Brain Mapp. 35(4):1681–1690.

Milner B. 1971. Interhemispheric differences in the localization of psychological processes in man. Br Med Bull. 27(3):272–277.

Mishkin M. 1982. A memory system in the monkey. Philos Trans R Soc Lond B Biol Sci. 298(1089):83–95.

Mitchell AS, Chakraborty S. 2013. What does the mediodorsal thalamus do? Front Syst Neurosci. 7(37):1–19.

Nichols EA, Kao YC, Verfaellie M, Gabrieli JD. 2006. Working memory and long-term memory for faces: evidence from fMRI and global amnesia for involvement of the medial temporal lobes. Hippocampus. 16(7):604–616.

Nystrom LE, Braver TS, Sabb FW, Delgado MR, Noll DC, Cohen JD. 2000. Working memory for letters, shapes, and locations: fMRI evidence against stimulus-based regional organization in human prefrontal cortex. Neuroimage. 11(5 Pt 1):424–446.

O'Reilly JX, Beckmann CF, Tomassini V, Ramnani N, Johansen-Berg H. 2010. Distinct and overlapping functional zones in

the cerebellum defined by resting state functional connectivity. Cereb Cortex. 20(4):953–965.

Ojemann G, Fedio P. 1968. Effect of stimulation of the human thalamus and parietal and temporal white matter on short-term memory. J Neurosurg. 29(1):51–59.

Ojemann GA, Blick KI, Ward AA Jr. 1971. Improvement and disturbance of short-term verbal memory with human ventrolateral thalamic stimulation. Brain. 94(2):225–240.

Olson IR, Moore KS, Stark M, Chatterjee A. 2006. Visual working memory is impaired when the medial temporal lobe is damaged. J Cogn Neurosci. 18(7):1087–1097.

Olson IR, Page K, Moore KS, Chatterjee A, Verfaellie M. 2006. Working memory for conjunctions relies on the medial temporal lobe. J Neurosci. 26(17):4596–4601.

Owen AM, Herrod NJ, Menon DK, Clark JC, Downey SP, Carpenter TA, Minhas PS, Turkheimer FE, Williams EJ, Robbins TW, et al. 1999. Redefining the functional organization of working memory processes within human lateral prefrontal cortex. Eur J Neurosci. 11(2):567–574.

Oztekin I, Davachi L, McElree B. 2010. Are representations in working memory distinct from representations in long-term memory? Neural evidence in support of a single store. Psychol Sci. 21(8):1123–1133.

Pardoe HR, Pell GS, Abbott DF, Jackson GD. 2009. Hippocampal volume assessment in temporal lobe epilepsy: how good is automated segmentation? Epilepsia. 50(12):2586–2592.

Parnaudeau S, O'Neill PK, Bolkan SS, Ward RD, Abbas AI, Roth BL, Balsam PD, Gordon JA, Kellendonk C. 2013. Inhibition of mediodorsal thalamus disrupts thalamofrontal connectivity and cognition. Neuron. 77(6):1151–1162.

Patenaude B, Smith SM, Kennedy DN, Jenkinson M. 2011. A Bayesian model of shape and appearance for subcortical brain segmentation. Neuroimage. 56(3):907–922.

Pergola G, Ranft A, Mathias K, Suchan B. 2013. The role of the thalamic nuclei in recognition memory accompanied by recall during encoding and retrieval: an fMRI study. Neuroimage. 74:195–208.

Pertzov Y, Miller TD, Gorgoraptis N, Caine D, Schott JM, Butler C, Husain M. 2013. Binding deficits in memory following medial temporal lobe damage in patients with voltage-gated potassium channel complex antibody-associated limbic encephalitis. Brain. 136(Pt 8):2474–2485.

Powell HW, Richardson MP, Symms MR, Boulby PA, Thompson PJ, Duncan JS, Koepp MJ. 2008. Preoperative fMRI predicts memory decline following anterior temporal lobe resection. J Neurol Neurosurg Psychiatry. 79(6):686–693.

Price GR, Mazzocco MM, Ansari D. 2013. Why mental arithmetic counts: brain activation during single digit arithmetic predicts high school math scores. J Neurosci. 33(1):156–163.

Ranganath C, D'Esposito M. 2001. Medial temporal lobe activity associated with active maintenance of novel information. Neuron. 31(5):865–873.

Romanski LM, Giguere M, Bates JF, Goldman-Rakic PS. 1997. Topographic organization of medial pulvinar connections with the prefrontal cortex in the rhesus monkey. J Comp Neurol. 379(3):313–332.

Rotshtein P, Soto D, Grecucci A, Geng JJ, Humphreys GW. 2011. The role of the pulvinar in resolving competition between memory and visual selection: a functional connectivity study. Neuropsychologia. 49(6):1544–1552.

Saalmann YB, Pinsk MA, Wang L, Li X, Kastner S. 2012. The pulvinar regulates information transmission between cortical areas based on attention demands. Science. 337(6095):753–756.

Seidenberg M, Hermann B, Pulsipher D, Morton J, Parrish J, Geary E, Guidotti L. 2008. Thalamic atrophy and cognition in unilateral temporal lobe epilepsy. J Int Neuropsychol Soc. 14(3):384–393.

Shallice T, Warrington EK. 1970. Independent functioning of verbal memory stores: a neuropsychological study. Q J Exp Psychol. 22(2):261–273.

Sherman SM, Guillery RW. 2011. Distinct functions for direct and transthalamic corticocortical connections. J Neurophysiol. 106(3):1068–1077.

Sinjab B, Martinian L, Sisodiya SM, Thom M. 2013. Regional thalamic neuropathology in patients with hippocampal sclerosis and epilepsy: a postmortem study. Epilepsia. 54(12):2125–2133.

Soei E, Koch B, Schwarz M, Daum I. 2008. Involvement of the human thalamus in relational and non-relational memory. Eur J Neurosci. 28(12):2533–2541.

Stewart CC, Griffith HR, Okonkwo OC, Martin RC, Knowlton RK, Richardson EJ, Hermann BP, Seidenberg M. 2009. Contributions of volumetrics of the hippocampus and thalamus to verbal memory in temporal lobe epilepsy patients. Brain Cogn. 69(1):65–72.

Sziklas V, Petrides M. 1999. The effects of lesions to the anterior thalamic nuclei on object-place associations in rats. Eur J Neurosci. 11(2):559–566.

Tanibuchi I, Goldman-Rakic PS. 2003. Dissociation of spatial-, object-, and sound-coding neurons in the mediodorsal nucleus of the primate thalamus. J Neurophysiol. 89(2):1067–1077.

Todd JJ, Marois R. 2004. Capacity limit of visual short-term memory in human posterior parietal cortex. Nature. 428 (6984):751–754.

Van der Werf YD, Scheltens P, Lindeboom J, Witter MP, Uylings HB, Jolles J. 2003. Deficits of memory, executive functioning and attention following infarction in the thalamus; a study of 22 cases with localised lesions. Neuropsychologia. 41(10):1330–1344.

Vertes RP, Hoover WB, Szigeti-Buck K, Leranth C. 2007. Nucleus reuniens of the midline thalamus: link between the medial prefrontal cortex and the hippocampus. Brain Res Bull. 71(6):601–609.

Voets NL, Zamboni G, Stokes MG, Carpenter K, Stacey R, Adcock JE. 2014. Aberrant functional connectivity in dissociable hippocampal networks is associated with deficits in memory. J Neurosci. 34(14):4920–4928.

Wager TD, Smith EE. 2003. Neuroimaging studies of working memory: a meta-analysis. Cogn Affect Behav Neurosci. 3(4):255–274.

Wickelgren WA. 1968. Sparing of short-term memory in an amnesic patient - implications for strength theory of memory. Neuropsychologia. 6(3):235.

Winocur G. 1985. The hippocampus and thalamus: their roles in short- and long-term memory and the effects of interference. Behav Brain Res. 16(2–3):135–152.

Yang T, Bavley RL, Fomalont K, Blomstrom KJ, Mitz AR, Turchi J, Rudebeck PH, Murray EA. 2014. Contributions of the hippocampus and entorhinal cortex to rapid visuomotor learning in rhesus monkeys. Hippocampus. 24(9):1102–1111.

Yonelinas AP. 2013. The hippocampus supports high-resolution binding in the service of perception, working memory and long-term memory. Behav Brain Res. 254:34–44.

Zarahn E, Rakitin B, Abela D, Flynn J, Stern Y. 2005. Positive evidence against human hippocampal involvement in working memory maintenance of familiar stimuli. Cereb Cortex. 15(3):303–316.